Available online at www.sciencedirect.com
SCIENCE DIRECT®
Nuclear Instruments and Methods in Physics Research A 499 (2003) 692–702
NUCLEAR INSTRUMENTS & METHODS IN PHYSICS RESEARCH Section A
www.elsevier.com/locate/nima

The laser system for the STAR time projection chamber

J. Abele[a], J. Berkovitz[a], J. Boehm[a], A. Brandin[b], E. Gushin[b], G. Harper[d], A. Lebedev[c,*], W.A. Love[c], A. Ridiger[b], M. Strikhanov[b], J Weidenbach[a], R. Wells[a], J. Wolf[a], J. Wirth[a], H.H. Wieman[a]

[a] *Lawrence Berkeley National Laboratory, Berkeley, CA 97420, USA*
[b] *Moscow Engineering Physics Institute, Moscow 115409, Russia*
[c] *Brookhaven National Laboratory, Upton, NY 11973, USA*
[d] *University of Washington, Seattle, WA 98195, USA*

Abstract

The Time Projection Chamber (TPC) is the core tracking detector for the STAR experiment at RHIC. To determine spatial distortions, calibrate and monitor the TPC, a laser calibration system has been built. We developed a novel design to produce ~500 thin laser beams simulating straight particle tracks in the TPC volume. The new approach is significantly simpler than the traditional ones, and provides a higher TPC coverage at a reduced cost. During RHIC 2000 and 2001 runs the laser system was used to monitor the TPC performance and measure drift velocity with ~0.02% accuracy. Additional runs were recorded with and without magnetic field to check $\mathbf{E} \times \mathbf{B}$ corrections.

PACS: 29.40.−n; 29.40.Gx

Keywords: Detectors; Laser; Time Projection Chamber; Calibration; Heavy ions

1. Introduction

Gas detectors in many modern experiments are large and complex. Assembling, testing, calibrating and monitoring during accelerator runs becomes a difficult task. The introduction of narrow ultraviolet (UV) laser beams to imitate straight charged particle tracks simplifies operating procedures [1]. If the laser beam position and time of appearance is known with high accuracy, repeated measurements provide precise calibration. Laser tracks have no multiple scattering and are not sensitive to magnetic fields. A comprehensive review of detector calibration by laser beams is presented in Ref. [2]. Experiments with gaseous detectors being proposed for new accelerators with much higher particle multiplicity foresee problems with two-particle resolution and distortion due to charge accumulation in the sensitive volume [3]. This becomes especially important at accelerators with high energy, heavy ion beams, where particle multiplicity could reach $dN/dy \sim 2000$–5000. To monitor these distortions, more calibration tracks are required. In this article we briefly describe the laser system for the Time Projection Chamber (TPC) in the STAR experiment at the heavy ion collider, RHIC [4].

*Corresponding author.
E-mail address: alebedev@bnl.gov (A. Lebedev).

0168-9002/03/$ - see front matter
PII: S0168-9002(02)01966-6

2. Laser system requirements

The main tracking detector in the STAR experiment is a TPC [5]. The task of the TPC is to provide track reconstruction, momentum measurement and particle identification. The STAR TPC is a cylinder 4 m in diameter and 4.2 m long, with a 0.5 T axial magnetic field. The TPC volume is bounded by coaxial inner and outer field cages (IFC, OFC) connected to end cap wheels with multiwire proportional chambers (MWPC) on the end wheels. The working gas for the MWPC is 90% argon and 10% methane (P-10). A high voltage membrane at the TPC center with resistor chains on the field cages creates a uniform electric field along the Z-axis (parallel to the magnetic field) in which electrons produced by charged particles drift to the end cap MWPCs. Measured drift time and the drift velocity provides the coordinate along Z, while induced signals on the pad rows provides spatial coordinates in the MWPC plane.

Physics goals for the STAR experiment impose 10% momentum resolution for a particle with a transverse momentum of 10 GeV/c. This requires an accuracy $\sim$200 μm in the sagitta measurement of the curved particle trajectory. The errors in the Z coordinate must be well under 1 mm. There are several sources of uncertainty in track coordinate measurements:

1. Variation in drift velocity caused by gas mixture, temperature, pressure and electric field variation.
2. TPC misalignment in the magnet and existence of the global $\mathbf{E} \times \mathbf{B}$ effect.
3. Radial inhomogenities of magnetic and electric field.
4. Space charge buildup due to high multiplicity in Au–Au collisions.
5. TPC endcap wheel displacement and inclination.

At maximum RHIC energy, Au–Au collisions create $\sim$2000 charged particles in the TPC volume which could produce charge accumulation and track distortions [6], especially near the IFC region at $\sim$0.6 m radius. These distortions varied significantly along the Z-axis in the TPC [3,6]. To see all spatial variations throughout the TPC volume it is desirable to increase the number of laser beams up to 100–400 for one-half TPC. Considering these issues we specified for the STAR laser system:

1. Number of laser tracks $\sim$100–400 in each half of the TPC.
2. Laser beams should fill the TPC volume uniformly.
3. Electron density along the laser beam in any point must be higher than ionization from relativistic particles.
4. The accuracy of the position and stability during operation of each laser beam at any point must be smaller than $\sim$200 μm in azimuthal and radial directions and smaller than $\sim$700 μm in axial direction.
5. Synchronization of the time of the laser beams appearance in the TPC volume to the RHIC clock within $\sim$5 ns error to provide $\sim$0.01% accuracy in drift velocity measurements.
6. Laser system must provide alignment, steering and stable position of laser beams with the accuracy specified above.

3. Laser system description

As shown in many investigations [2,7], UV-laser beams produce ionization in gaseous detectors via a two-photon ionization process of organic substances, which are commonly present in the detector volume at $\sim$ppb level. A Nd-YAG frequency-quadrupled laser ($\lambda = 266$ nm) with energy density about 1–20 μJ/mm^2 can produce ionization equivalent to a relativistic particle (mip) in common gases without special additives.

There are two optics designs widely used to produce multiple narrow laser beams. In the first design a powerful laser beam is focused by a demagnification telescope to $\sim$1 mm diameter beam with the smallest waist positioned in the detector center. This beam is split by semitransparent mirrors, installed on an inner surface of the detector (ALEPH TPC [8]), or on a separate optical bench near the detector (EOS TPC [9]). There are several difficulties in this design. The

number of narrow beams is limited by mirror coating resistance to laser radiation. The safe energy level for dielectric coating and UV radiation is $\sim 0.1\,J/cm^2$ [10], so only ~ 100 laser beams could be formed by one laser. It is also difficult to produce approximately equal beam intensity by splitting a single laser beam through multiple mirror stacks. In a second design a low power laser beam is focused by the previous method. This beam is then directed by steering mirrors into the TPC volume in different directions. The difficulty with power density is replaced by stringent requirements on stability and repeatability of mechanical drivers for the steering mirrors. For a detector with the size $\sim 5\,m$ and laser beam stability on the level of $\sim 100\,\mu m$, the angular movement of the mirror must be controlled to $<10^{-5}$ rad. This approach also significantly increases the time required to provide full chamber calibration. This kind of laser system was used in the OPAL jet chamber [11], the NA49 TPC [12] and the CERES TPC.

We proposed a novel design to produce a large number of narrow laser beams by splitting a wide laser beam with a diameter ~ 20–$30\,mm$ by many small diameter mirrors, installed in a region of approximately equal intensity. Small mirrors are made from glass rods, cut at 45°, polished and covered by dielectric coating with 100% reflectivity (Fig. 1). More effective use of the wide laser beam is accomplished by gathering the small mirrors in bundles; in our design there are 7 small mirrors in each bundle. Each mirror in a bundle is rotated to create different directions for the calibration beams in the TPC volume.

The creation of a thin beam by each small mirror is the same as the diffraction of the plane wave through a small circular aperture [13]. The spread and size of the diffraction pattern is defined by the Fresnel number $N = a^2/\lambda z$, where a is the aperture radius, λ the wavelength of the laser light and z is the distance from the aperture to the viewer. For $N<1$ the so-called Airy-disc diffraction pattern is created. For 0.5 mm radius and $\lambda = 266\,nm$, $N<1$ if $z>1\,m$. The divergence of the Airy disc, $\theta = 1.22\lambda/2a$, is comparable with divergence of the beam from focusing telescopes, $\theta = \lambda/\pi a$ (~ 0.17 mrad for $a = 0.5\,mm$). In the near field region, when the Fresnel number $N = d^2/4\lambda z > 1$ ($z<1\,m$) the laser beam is confined in a ~ 1 mm diameter cylinder.

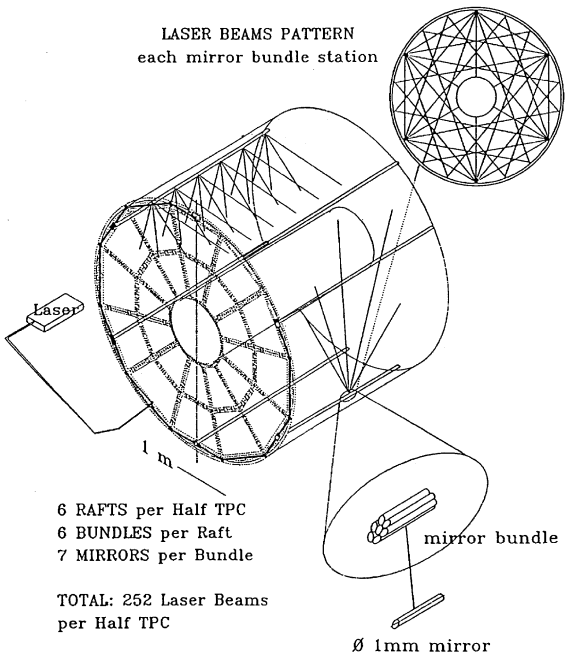

Fig. 1. Conceptual design of the laser system.

The production of thin laser beams by single small mirrors installed in wide laser beam was used in the laser calibration system for the 1.5 m streamer chamber of the magnetic spectrometer SCAP (IHEP) [14].

The advantage of the design is that the initial point in space of each thin laser beam is completely defined by the position of the small mirror and only deflection of the wide beam could change the direction of the thin beam. One half of the laser system is presented schematically in Fig. 2. The Nd:YAG laser GCR-130-10 [15] operates in Q-switched mode to obtain high power laser pulses of ~ 3–$4\,ns$ duration. A Glan-laser polarizer and rotating half-wave plate are used to change the laser power over a wide range to produce calibration beams with different ionization. The laser beam is expanded by a telescope to $\sim 30\,mm$ diameter and directed to the TPC endcap wheel through a hole in the magnet steel. On the TPC outer radius a system of dielectric splitters

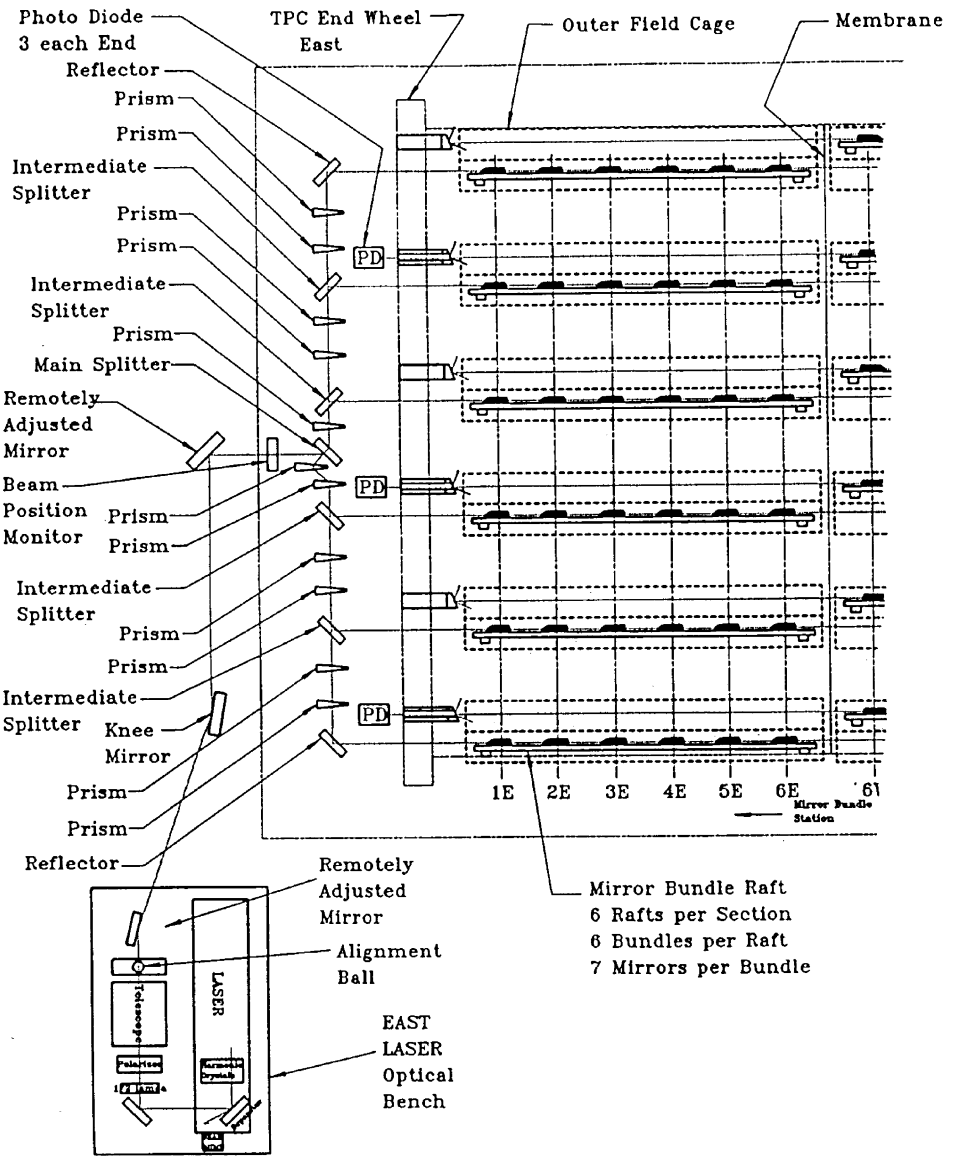

Fig. 2. Optical scheme for one-half TPC.

and prisms are installed to rotate and split the wide beam into 6 beams with equal intensity. These beams are directed to positions 60° apart along the inner surface of the OFC parallel to the Z-axis of the TPC. There are 6 rafts installed parallel to the laser beams. Square glass tubes ~ 1500 mm length were used for the raft as a rigid and stable support for mirror bundles. Three-ball supports are glued to each raft to decrease the influence of OFC distortions. Six bundles are installed on each raft ~ 300 mm apart and uniformly occupy the wide beam. These bundles produce seven different directions of thin laser beams, covering approximately uniformly the whole TPC volume. This design provides $(6 \times 6 \times 7 = 252)$ laser calibration beams for each half of the TPC. In addition, the

residual beam, which survives after passing through the raft, is directed through a slot in the central membrane towards diffuse reflectors, installed on the opposite TPC wheel. Reflected from these diffusers, UV light illuminates the central membrane, which is made from carbonized kapton with a pattern of 3 mm wide aluminum stripes glued on. Electron clouds emitted from the stripes by a one-photon ionization process provide signals similar to the laser beams in the TPC volume. The membrane pattern covers all the TPC sectors at the maximum drift distance and was used to align TPC sectors.

4. Laser subsystems

4.1. Bundle production

The main element in this system is the bundle of small mirrors. We produced small mirrors with different diameters (Fig. 3) to determine beam formation, technology and assembly procedures. A mirror smaller than 1 mm diameter creates significant divergence, and difficulties with production and alignment. Bigger diameter required wider beams, increased laser power and optics sizes. We therefore chose 1 mm as the basic diameter for mirrors to produce thin beams with good quality up to 4 m. A support was designed to install and adjust the position and angle of each 1 mm mirror in a bundle. The mirrors were then glued together in a metal collar. Two sets of mirror angles were used to provide more uniform TPC coverage. The relative mirror position in each bundle was measured with an accuracy $\sim 30\,\mu m$. A special installation was developed to measure all angles between mirror faces. A vertically aligned wide laser beam shines on the bundle, installed on the top of a theodolite. Reflected thin laser beams are directed to a quadrant detector, installed on a vertical stage. The position of the beam was determined with $\sim 100\,\mu m$ accuracy at 4 m distance from the theodolite, and an accuracy of ~ 0.025 mrad for the horizontal angle was achieved, while the vertical angle was measured by the stage with an accuracy ~ 0.12 mrad. After these measurements, the bundles were assembled on the raft, the position of each bundle was measured with $\sim 100\,\mu m$ accuracy and 12 rafts with bundles were aligned inside the TPC volume. Finally, the position of each mirror in the TPC coordinate system was measured with $\sim 200\,\mu m$ accuracy.

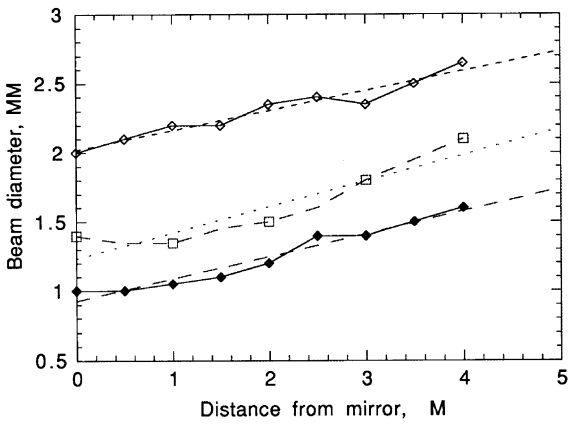

Fig. 3. The formation of thin laser beams by small mirrors.

4.2. Laser beam characteristics

Linear electron density along the laser beam was measured by a drift chamber filled by P-10 gas with a 2 cm sensitive region along the anode wire.

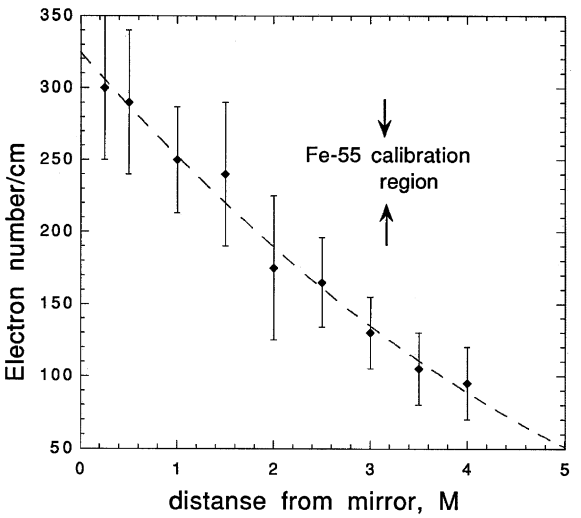

Fig. 4. Linear electron density from a laser beam created by a 1 mm mirror.

The laser beam was directed parallel to the anode wire, entering the drift volume through a quartz window. The linear electron density at distances up to 4 m from the 1 mm diameter mirror is shown in Fig. 4. A laser power density of ~ 1–$2\,\mu J/mm^2$ was enough to produce ionization close to mip. Due to the quadratic dependence of two-photon ionization on the power density we can estimate the "electron" divergence of a laser beam in a drift chamber assuming uniform power density across the laser beam. Assume N_p is the number of photons in a laser beam with diameter $d = d_0 + \alpha M$, N_e is the linear electron density and M is the distance from the drift chamber to the small mirror. Then $N_e = N_p^2/S$, where S is the beam area, $S = \pi d^2/4$, and for N_p-const, $N_e \sim 1/(d_0 + \alpha M)^2$. A fit from experimental data yields an "electron" divergence $\alpha = (0.16 \pm 0.04)$ mrad, which is close to the optical divergence, $\theta = 2\lambda/\pi d$ (~ 0.17 mrad for $d = 1$ mm).

The total number of laser beams is determined by the wide laser beam area and the number of bundles occupying it. Bundles are installed along the Z-axis about 30 cm apart. Diffraction from the bundle supports could distort the uniformity of the wide laser beam, so we investigated the influence of the transverse distance between bundles on a raft on the thin laser beam position and electron density. For distances smaller than 0.5 mm, linear electron density starts to decrease. For reliability and ease of adjustment a 1 mm radial distance between bundles was chosen. At this distance no laser beam disturbance was observed.

4.3. Monitoring and beam steering

Remote laser operation used the global TPC operations slow control infrastructure. A graphical user interface (GUI), accessible on a PC in the STAR control room using EPICS [21] (Fig. 5a) provides start–stop procedures for the selected laser and defines run time. The Poisson line reference method [16] was chosen to perform positioning and steering of the wide laser beam. After the expanding telescope a 3 mm ball is installed in the center of the wide laser beam

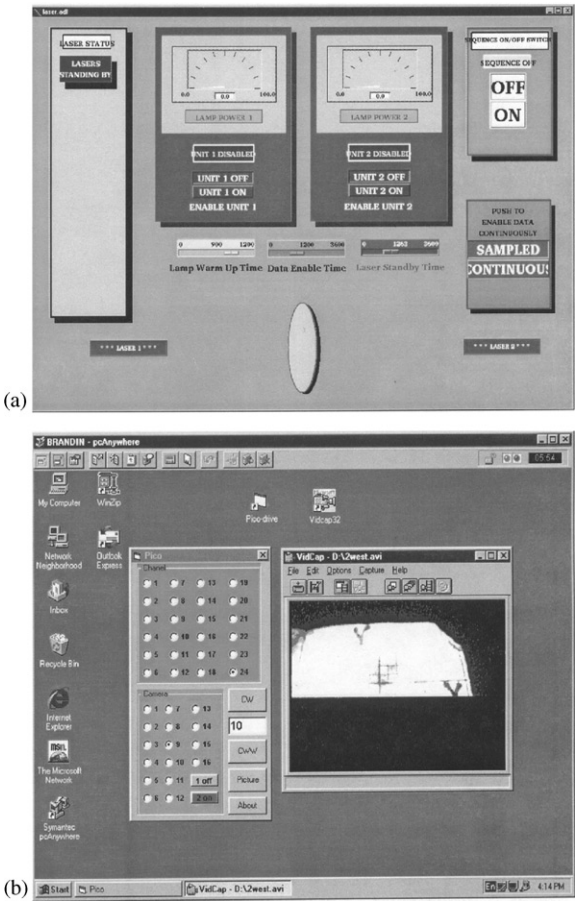

Fig. 5. Remote computer windows to operate the laser system: (a) control window for laser operation, (b) window to align and monitor laser beams.

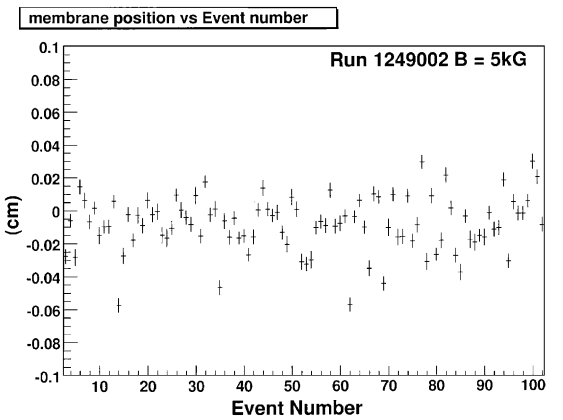

Fig. 6. The membrane position stability using a trigger synchronized with the RHIC clock.

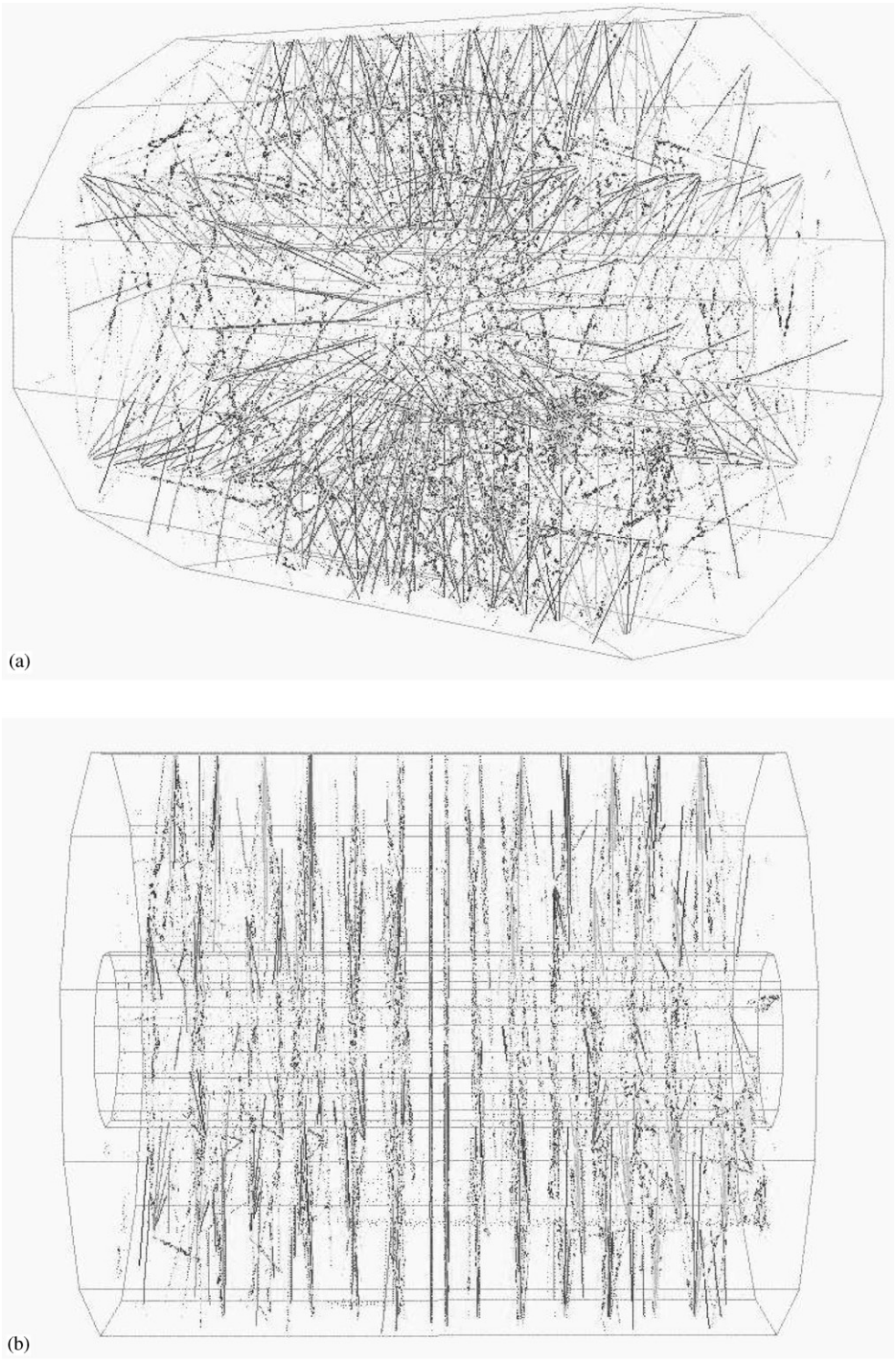

Fig. 7. Laser event in TPC: (a) perspective view, note the radial lines from membrane in the TPC center, (b) side view.

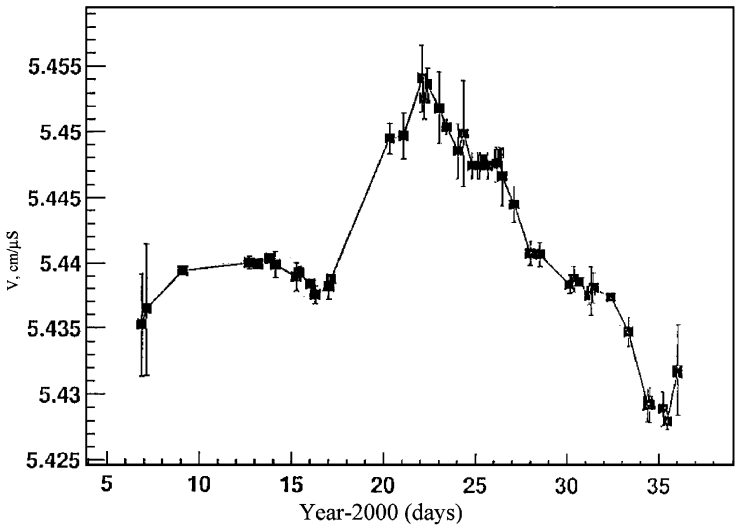

Fig. 8. Laser drift velocity measurement over one month during year 2000.

(Fig. 2). In the center of the dark shadow a bright spot appears, and a very thin "Poisson beam" is created. The divergence of this "Poisson beam" is extremely small, ~0.05 mrad at 266 nm wavelength. A quadrant detector or CCD camera could easily monitor this beam. The quadrant detector is workable only with an additional diaphragm, cutting the bright field of wide beam, and this circumstance decreases the region of steering operation for wide beam by ~1 mm. A miniature CMOS CCD camera (type MC-MRB-4 [17]) with lens and fluorescence screen ~20 mm diameter was chosen to pick up the laser beam image. This camera could work in 1.0 T magnetic field. The screen has a mm scale grid, so viewing and alignment of the laser beam becomes a convenient procedure. Compact piezoelectric picomotor drivers were chosen [18] to provide mirror adjustment. The driver has a resolution <0.1 μm, minimum backlash and insensitivity to magnetic field. Remote control over the piezodrives and CCD cameras was installed on a PC computer. Another GUI (Fig. 5b) was used to provide observation of the laser beam through the set of four CCD cameras installed on the TPC and operation of 24 piezodrivers to monitor and align the laser beam with ~200 μm accuracy. This system was used to correct shifts of the laser beam position due to magnetic forces. From zero to full field the position of laser beam at the TPC entrance shifted up to 3 mm.

4.4. Laser trigger

The laser operation frequency is (10±0.5) Hz. A TTL pulse triggers the xenon lamps to pump the YAG crystal and after ~180 μs a second TTL pulse provides Q-switch opening. After ~30–40 ns an UV pulse is emitted from the laser. A signal from a photodiode is used as a start signal for TPC readout. STAR detectors were synchronized with the RHIC clock (~10 MHz). The laser trigger board accepts an external RHIC clock signal and provides, simultaneously for both lasers, a trigger for the lamp and Q-switch synchronized with the RHIC clock with a jitter ~5–6 ns. In Fig. 6 the mean position of the central membrane, measured by electrons from the Al stripes, for the synchronized laser is presented. We achieved an accuracy ~200 μm in determining Z-coordinates, which affects the error in drift velocity measurement.

5. RHIC runs results

The laser calibration system was used extensively during TPC test runs with cosmic rays starting in 1997. Reconstruction of the laser events

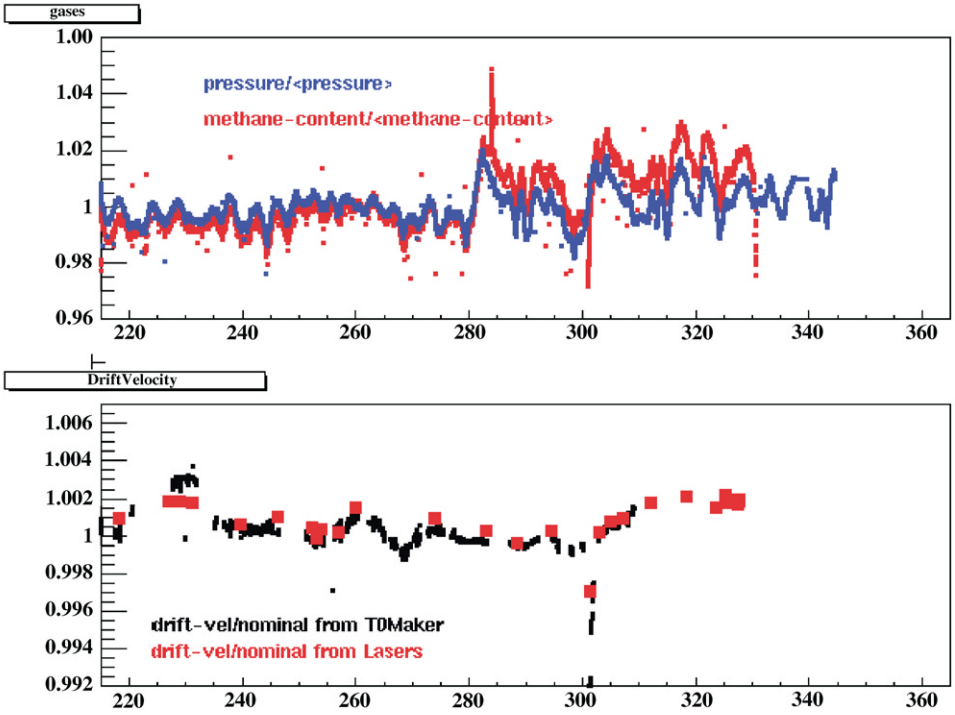

Fig. 9. A comparison of laser drift velocity measurements for year 2001–02 using the laser system and by matching TPC vertices from each half (T0Maker). The top panel shows the variations of the TPC pressure and methane content for the same period.

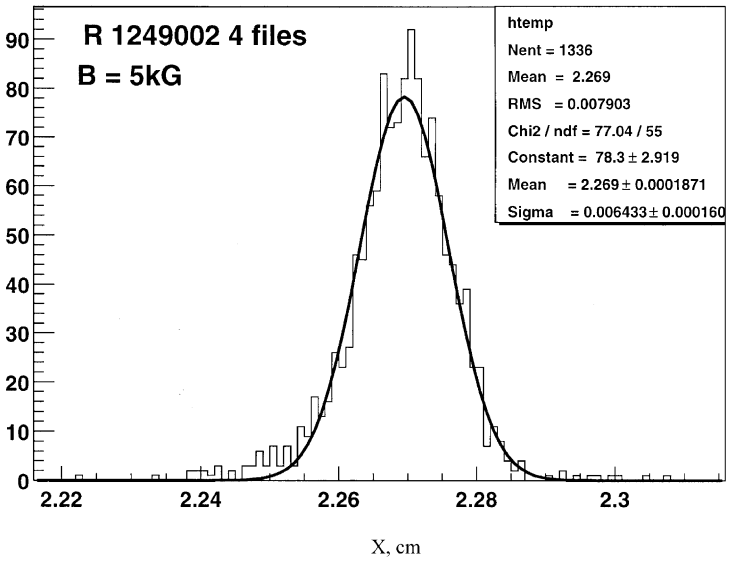

Fig. 10. Pointing stability of laser tracks.

helped to recognize errors in tracking code, wrong cabling and non-functioning readout electronics. Laser data were used to align the inner and outer sectors. Also lasers were used to check the clock frequency by matching the membrane image for both TPC halves.

During the summer of 2000 about 80 laser calibration runs were recorded. Precise drift velocity measurement is crucial for physics analysis and to match tracks across TPC halves. For each physics run a laser calibration run was recorded, containing ~ 500 events. A typical laser event with different projection views is presented in Fig. 7. Approximately 450 laser tracks are recorded in a single event. Radial lines in the TPC center are the image of the Al stripes on the central membrane. For analysis of this event a time offset of ~ 500 ns was used to separate the central membrane images for display.

A drift velocity was determined using the Z position difference of the mirror positions for the sets of laser tracks closest to and furthest from the pad plane. Tracks were extrapolated to the mirror's X, Y position and the ratio of the measured dZ and the survey dZ was used to scale the input velocity. In Fig. 8 the laser-measured drift velocity monitored over a one month period is shown. There are several parameters affecting drift velocity: barometric pressure, cathode voltage, temperature, clock frequency, methane concentration and unknown additives in TPC gas. We estimate that the most influential parameter is methane concentration. To check systematic error in our data the ratio $R = W(\text{east})/W(\text{west})$ was calculated, where W(east) and W(west) are data for two TPC halves. For all laser runs $R = 0.999991 \pm 0.000225$.

In addition to using the laser system, the drift velocity in TPC could be calibrated by matching the primary vertices reconstructed independently in each half of the TPC. This method works best for high multiplicity events and is not usable for low multiplicity events such as p + p collisions. For p + p runs, the laser drift velocity calibration was used exclusively. During RHIC 2001–02 run, a special trigger was implemented to interleave laser events in a physics run, and a comparison of the two methods of drift velocity determination is shown in Fig. 9. On-line software provides a fast calculation of drift velocity using the laser triggers, and these results are monitored to look for problems with TPC gas. The dip in the drift velocity near day 300 caused by a temporary methane loss in the gas system.

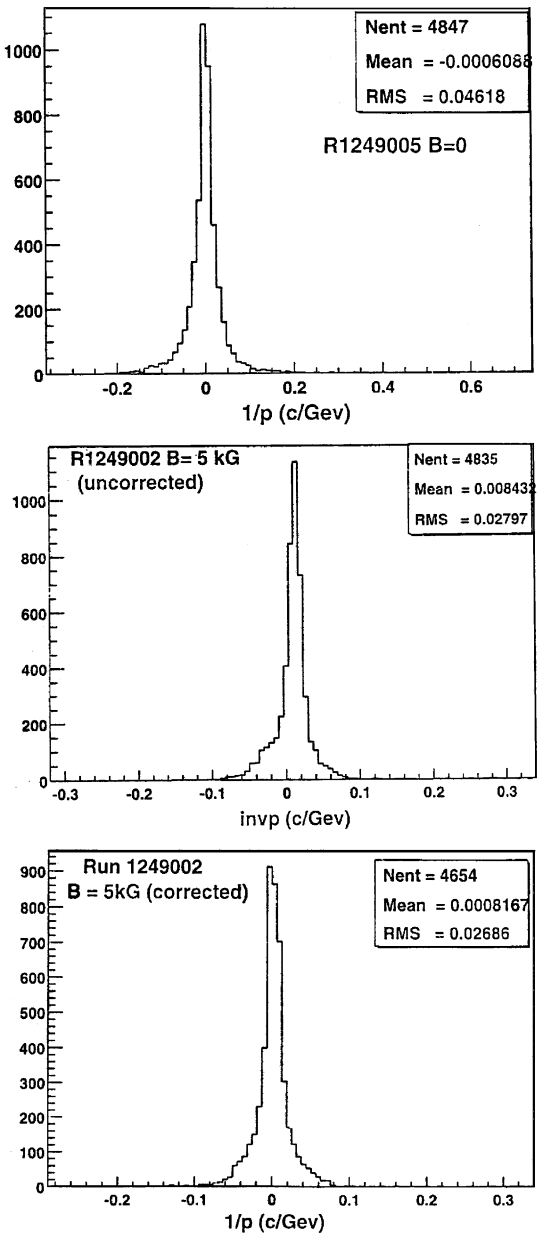

Fig. 11. Histograms of inverse momentum distribution for radial laser tracks: $B = 0$, $B = 0.5$ T (no $\mathbf{E} \times \mathbf{B}$ corrections), $B = 0.5$ T (corrected for $\mathbf{E} \times \mathbf{B}$ distortion).

We measured the position stability of laser beams to understand the limits of accuracy of the system. Fig. 10 shows a histogram of transverse position for a powerful laser beam with ionization ~ 10 mip. The error (sigma) on the level of $\sim 64\,\mu m$ confirms our expectations about laser track stability. For a laser with ionization ~ 1–2 mip, stability is ~ 150–$200\,\mu m$.

The momentum resolution of the TPC is defined by accuracy in sagitta measurement and multiple scattering. For high momentum tracks the influence of multiple scattering is negligible. For high momentum the resolution is $dp/p = Ap/B$ [19], where p is the particle transverse momentum, B-the magnetic field and A is the error in sagitta measurement. There are several factors affecting A: the track length, the accuracy in point measurement on the particle trajectory and the number and the position of these points. Laser tracks, which could be represented as particles with infinite momentum, are an excellent tool to determine all these errors. Distribution of inverse momentum $f = 1/p$ for radial laser tracks provides systematic effects, a limit in determining particle momentum and TPC momentum resolution. The width of the histogram f, $df = (dp/p)1/p$ provides a direct value of A. Data without B field represents systematic error in global reconstruction. Although extensive and detailed $\mathbf{E} \times \mathbf{B}$ corrections were made with particles from central Au–Au collisions, it is useful to check these corrections with laser tracks. Fig. 11 shows corrected and uncorrected f-distributions. The data shows small systematic errors and the ability to measure particle momentum with designed accuracy.

An upgrade for the laser system foreseen in the near future is a fully automated system to monitor and align lasers for the TPC and a calibration procedure for another tracking detector in STAR—the Forward TPC (FTPC) [20].

6. Summary

The results reported here show the durability of the STAR TPC laser calibration system. During the RHIC 2000 and 2001–02 runs the laser system was used to measure the drift velocity with $\sim 0.02\%$ accuracy and monitor the stability of the TPC electronics. This system was expanded to calibrate and monitor Forward Time Projection Chambers. Further improvements in TPC global position accuracy will be implemented with more laser data.

Acknowledgements

This work was supported by US Department of Energy, Ministry of Education, Ministry of Science, Russian Federation.

References

[1] M. Anderhub, M.J. Devereux, P.G. Seiler, Nucl. Instr. and Meth. 166 (1979) 581.
[2] H.J. Hilke, Nucl. Instr. and Meth. A 252 (1986) 169.
[3] ALICE Technical Design Report, CERN/LHCC 2000-001 7 January 2000.
[4] J. Harris, et al., Nucl. Phys. A 566 (1994) 277.
[5] H. Wieman, STAR collaboration, IEEE Trans. NS-44 N3 (1997) 671.
[6] G. Ray, STAR note #0003, LBL, 1992 (see www.star.bnl.gov).
[7] E.M. Gushchin, A.N. Lebedev, S.V. Somov, Nucl. Instr. and Meth. 228 (1984) 94.
[8] W.B. Atwood, et al., Nucl. Instr. and Meth. A 306 (1991) 446.
[9] H. Wieman, et al., Nucl. Phys. A 525 (1991) 617.
[10] Newport Corporation, Inc.catalog, Irvine, CA, 92713, 1994, p. 2.25
[11] O. Biebel, B. Boden, H. Borner, et al., Nucl. Instr. and Meth. A 320 (1992) 183.
[12] R. Reinfordt, Frankfurt University, private communication
[13] A. Siegman, Lasers, University Science Books, 1986, p.728.
[14] E.M. Gushchin, A.N. Lebedev, V.A. Ryabov, et al., Prib. Tekh. Exp. N4 (1990) 63 (in Russian).
[15] Spectra-Physics Lasers, Inc, http://www.splasers.com.
[16] L.V. Griffith, et al., Rev. Sci. Instr. 61 (N8) (1990) 2138.
[17] WellchAllyn, Data Collection Division, http://www.wellchallyn.com.
[18] New Focus, Inc., http://www.newfocus.com.
[19] W. Blum, L. Rolandi, Particle Detection with Drift Chambers, Springer, Berlin, 1994.
[20] F. Bieser, V. Eckardt, et al., The Forward Time Projection Chamber for the STAR Detector. MPI-PhE/98-3, 1998.
[21] D. Rechhold, et al., Hardware control for the STAR experiment at RHIC, Nucl. Instr. and Meth. A (2003) this volume.

This page intentionally left blank